

Knowledge-guided machine learning for county-level corn yield prediction under drought

Xiaoyu Wang^a, Yijia Xu^a, Jingyi Huang^b, Zhengwei Yang^c, Zhou Zhang^a

^a*Biological Systems Engineering, University of Wisconsin-Madison, Madison, 53706, WI, USA*

^b*Department of Soil and Environmental Sciences, University of Wisconsin-Madison, Madison, 53706, WI, USA*

^c*Research and Development Division, National Agricultural Statistics Service, United States Department of Agriculture, Washington, 20250, DC, USA*

Abstract

Remote sensing (RS) technique, enabling the non-contact acquisition of extensive ground observations, is a valuable tool for crop yield predictions. Traditional process-based models struggle to incorporate large volumes of RS data, and most users lack understanding of crop growth mechanisms. In contrast, machine learning (ML) models are often criticized as “black boxes” due to their limited interpretability. To address these limitations, we utilized Knowledge-Guided Machine Learning (KGML), a framework that leverages the strengths of both process-based and ML models. Existing works have either overlooked the role of soil moisture in corn growth or did not embed this effect into their models. To bridge this gap, we developed the Knowledge-Guided Machine Learning with Soil Moisture (KGML-SM) framework, treating soil moisture as an intermediate variable in corn growth to emphasize its key role in plant development. Additionally, based on the

prior knowledge that the model may overestimate under drought conditions, we designed a drought-aware loss function that penalized predicted yield in drought-affected areas. Our experiments showed that the KGML-SM model outperformed other traditional ML models. We explored the relationships between drought, soil moisture, and corn yield prediction by assessing the importance of different features within the model, and analyzing how soil moisture impacts predictions across different regions and time periods. Finally we provided interpretability for prediction errors to guide future model optimization.

Keywords: Corn yield prediction; Knowledge-guided Machine learning; Soil moisture; drought-aware learning

1. Introduction

Corn, as a primary crop, plays a vital role in the U.S. agriculture, supporting food security as well as the animal feed and biofuel industries (Graham et al., 2007; Thompson, 1969). Accurate yield prediction is crucial for effective resource management and economic stability (Kucharik and Ramanakutty, 2005). Achieving accurate prediction across large areas and diverse environmental conditions is challenging (Weiss et al., 2020). Traditional process-based models (Weiss et al., 2007) are built on a deep understanding of the physical, chemical, and biological processes within crop growth systems (Weiss et al., 2004). These models use equations derived from scientific principles to simulate the behavior of crops, weather, and soil interactions (Weiss et al., 2002), making them highly interpretable and reliable in scenarios where the underlying processes are well understood (Puntel et al., 2016;

Shahhosseini et al., 2021). Several promising modeling frameworks are designed for simulating and predicting agricultural production systems, such as the Agricultural Production Systems sIMulator (APSIM) (McCown et al., 1996), the Decision Support System for Agrotechnology Transfer (DSSAT) (Jones et al., 2003), the WOWorld FOod STudies (WOFOST) (Van Diepen et al., 1989), and the Agricultural Policy / Environmental eXtender (APEX) (Williams and Izaurrealde, 2010). Many studies (Zhen et al., 2023, 2022) have successfully used these models to predict crop yields. However, process-based models have several limitations. Plant growth is highly complex, and these models rely on a limited set of fixed input features, which are insufficient to accurately capture the intricacies of this process. Moreover, process-based models require extensive manual parameter tuning, limiting their applicability for applications across vast regions.

In recent years, remote sensing (RS) has provided several benefits for corn yield prediction (Lobell et al., 2015). It enables the collection of large-scale real-time data across vast agricultural areas. This data, typically combined with machine learning (ML), facilitates accurate and efficient large-scale yield prediction. Deep learning (DL) (Goodfellow et al., 2016), a widely used ML method, has the advantage of leveraging a large amount of RS data by automatically learning features from big datasets. This removes the need for manual feature engineering, enabling the model to capture complex patterns and relationships between crop environmental factors and crop yield (He et al., 2016). Many studies applying DL to crop yield prediction have shown its advantages in performance improvement. You et al. (2017) introduced a scalable approach to crop yield prediction using modern representation

learning rather than traditional hand-crafted features, achieving impressive results. [Wang et al. \(2018\)](#) demonstrated soybean yield predictions in Argentina and obtained reliable results in Brazil using transfer learning, even with limited data. [Ma et al. \(2021a\)](#) developed a county-level corn yield prediction model using a Bayesian Neural Network across 12 states in the Corn Belt, showing the potential for large-scale corn yield prediction tasks. However, despite the popularity of DL models in corn yield prediction tasks, they have certain limitations. First, DL models require a large amount of data to learn the relationships between inputs and outputs. Additionally, DL models often function as a black box, lacking reliable interpretability of the prediction results. Specifically, crop growth involves complex biological processes among soil, weather, and corn, which are challenging for DL models to fully capture. Therefore, how to leverage advantages of process-based models and DL models to address these challenges has become an important research topic.

Knowledge-guided machine learning (KGML) ([Karpatne et al., 2022](#)) aims to integrate scientific knowledge in ML frameworks to achieve better performance, scientific consistency, and explainability of results. KGML involves three main approaches: Knowledge-Guided Learning, Knowledge-Guided Architecture, and Knowledge-Guided Pretraining. Knowledge-Guided Learning incorporates scientific knowledge, such as physical laws, into the learning algorithm by modifying the loss function. It guides the optimization process toward scientifically consistent and generalizable solutions ([Daw et al., 2022](#); [Bao et al., 2021](#)). Knowledge-Guided Architecture embeds scientific knowledge directly into the structure of the ML model. By designing knowledge-

guided neural network architectures, researchers can enable models to automatically capture physical properties or conservation laws, which improves both interpretability and robustness (Dugdale et al., 2017; Luo et al., 2023). Knowledge-Guided Pretraining uses simulated data or self-supervised learning tasks to pretrain ML models. By initializing model parameters using data that encodes scientific principles, this method reduces the need for large amounts of observational data and improves performance in data-scarce scenarios (Licheng et al., 2022; Chen et al., 2023). Building on these approaches, KGML has been increasingly used in various domains, such as agriculture, hydrology, and biology, enabling improved data-driven decision-making and predictive modeling.

Recently, many studies have used KGML to combine process-based and ML models for crop yield predictions (Kimball et al., 2023; Burroughs et al., 2023). Since process-based models already provide insights into the crop growth process and generate high-quality simulated data, Knowledge-Guided Pretraining is the most popular approach (He et al., 2023; Yang et al., 2023). These studies aim to identify patterns between agricultural features and crop yields from large datasets using ML, while leveraging data simulated by process-based models to provide interpretability. Specifically, intermediate variables in crop growth generated by process-based models are used to train ML models, allowing the ML models to simulate specific parts of the crop growth process. For example, He et al. (2023) integrated physical knowledge from process-based models and enabled the model to adjust for temporal data shifts over the years. Yang et al. (2023) used both historical and in-season RS data to better predict key agricultural variables such

as grain yield and carbon cycling processes. [Yang et al. \(2024\)](#) presented a knowledge-guided computer vision framework designed to monitor and simulate the growth of individual strawberry fruits, which can predict growth at the individual fruit level by integrating image-based data and dynamic simulations.

Although these KGML models have made significant progress in crop yield prediction, all existing KGML-based studies on crop yield predictions have overlooked the critical role of soil, particularly how soil moisture contributes to corn growth and affects yield. Soil moisture is influenced by temperature, precipitation, and other environmental factors and directly affects crop growth. As a key indicator of crop water supply, low soil moisture causes water stress, which limits corn growth and reduces yields ([Unganai and Kogan, 1998](#)). Unlike most RS data, such as NDVI, which only reflects the growth status of plants at a specific moment, soil moisture has a cumulative impact on yield over time. Nonetheless, a significant challenge for ML models is the limited availability of soil moisture data. For example, the widely used SPL4SMGP.007 SMAP soil moisture dataset ([Reichle et al., 2022](#)) only covers the period from 2015 onward, which limits the ability of ML models to learn from extensive historical data and impacts model performance. Therefore, we present a Knowledge-Guided Machine Learning with Soil Moisture (KGML-SM) framework that explicitly incorporated the soil moisture impact in the ML model and provided interpretability. The model consisted of two major components: a Weather-to-Soil (W2S) encoder modeling the relationship between weather inputs and soil moisture outputs, and an attention module ([Vaswani, 2017](#)) integrating features from multiple sources and dy-

namically weighting their influences on corn yield across time and space. To train this model, we adopted a two-step process. First, we used the APSIM model to generate a simulated field-level dataset for pretraining. Then, the model was finetuned using a county-level dataset from Google Earth Engine (GEE) (Gorelick et al., 2017) and United States Department of Agriculture (USDA) National Agricultural Statistics Service (NASS).

Furthermore, we conducted research into the relationship between soil moisture and corn yield prediction in drought-affected areas, where drought often reduced yields and caused overestimation (Cooper et al., 2014). Researchers have long been interested in studying the relationship between soil moisture, drought, and corn yield prediction (Ines et al., 2013; Bushong et al., 2016; Mladenova et al., 2017). However, these studies either had a narrow scope, or did not utilize this connection for model optimization. we designed a drought-aware loss function to further enhance model performance under drought conditions and mitigate overestimation problem. Finally, based on the relationship between soil moisture and corn yield prediction, we provided explanations for the prediction errors of the KGML-SM model and offered directions for future model optimization. Our research aimed to improve the accuracy and interpretability of corn yield predictions, ultimately contributing to more resilient agricultural systems under extreme weather variability.

Our main contributions are as follows:

- This paper introduced the KGML-SM framework. This framework integrated process-based and ML models for corn yield prediction while explicitly incorporating the influence of soil moisture.

- A drought-aware loss function was designed. This function enhanced model performance under drought conditions and mitigated overestimation.
- Based on the relationship between drought, soil moisture, and corn yield prediction, we provided interpretability for the prediction errors of the KGML-SM model and offered directions for future model optimization.

2. Data acquisition

In this study, we developed two datasets for corn yield prediction. The first dataset was a field-level dataset generated using APSIM (McCown et al., 1996) and used for pretraining. The second dataset was a county-level dataset derived from GEE (Gorelick et al., 2017) and USDA NASS and used for finetuning. The workflow was divided into three main steps: simulation, pretraining, and finetuning. A summary of all public datasets used in this study is provided in Table 1. In this section, we first introduce the study area (Sec. 2.1); then, we provide details of the APSIM field-level dataset (Sec. 2.2); finally, we describe the construction of the GEE county-level dataset (Sec. 2.3).

Table 1: Public datasets used in this study. a, b, and c indicate different purposes: a for APSIM simulation, b for model pretraining, and c for model finetuning.

Dataset	Use	Description	References
Iowa Environmental Mesonet	a, b	In-situ weather data	(Herzmann et al., 2004)
PRISM	c	Gridded weather data	(Daly et al., 2015, 2008)
MODIS MCD43A4	c	Vegetation indices	(Schaaf and Wang, 2015)
MODIS MCD18A1.061	c	Radiation data	(Wang, 2021)
USDA-CDL	c	Crop data layer	(USDA-NASS, 2017)
SMAP	c	Soil moisture data	(Reichle et al., 2022)
USDA NASS yield	c	County-level yield	(USDA, 2020)

2.1. Study area

Our research focused on corn yield prediction across the U.S. Corn Belt. Twelve states are selected as our study area, including North Dakota, South Dakota, Minnesota, Wisconsin, Iowa, Illinois, Indiana, Ohio, Missouri, Kansas, Nebraska, and Michigan. These states are crucial agricultural states in the U.S., known for their significant contributions to corn production. We generated a five-year average yield map (Fig. 1) for these twelve states and considered them well suited for corn yield prediction research.

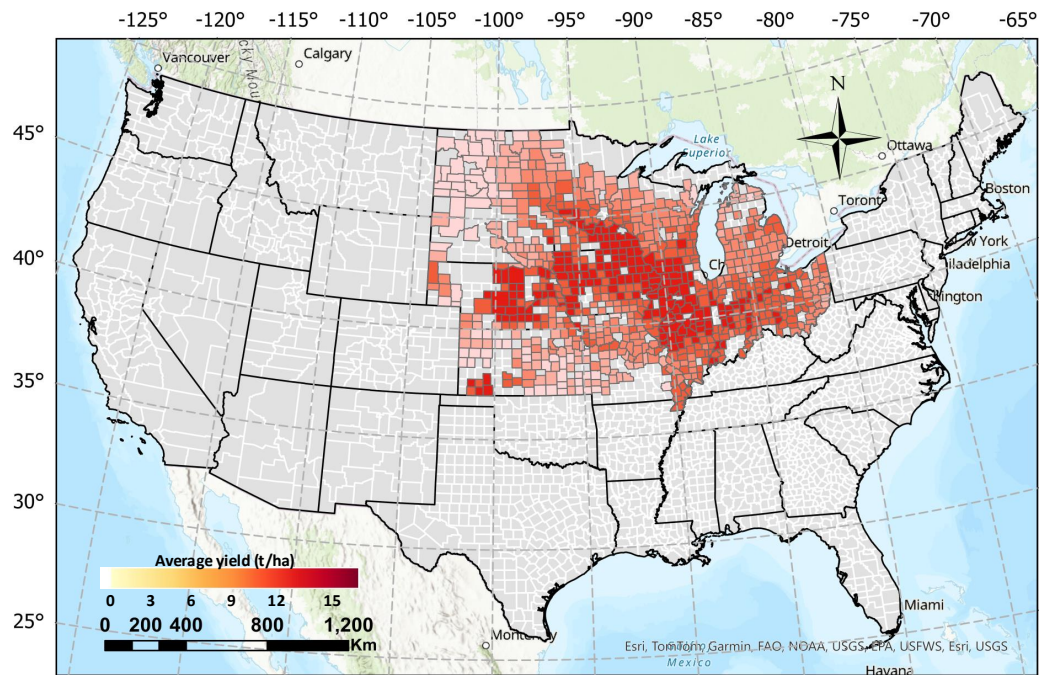


Figure 1: The 5-year average county-level corn yield map in selected states.

2.2. APSIM field-level dataset

In this section, we explain how APSIM was used to generate a field-level simulated dataset for model pretraining. We used data from the Iowa Environmental Mesonet (IEM) (Herzmann et al., 2004), a platform developed by Iowa State University that provides U.S. agricultural and environmental data. We extracted all available station data from the IEM, which included data from thousands of stations across 12 states from 1980 to 2023 (Table 2).

Table 2: The number of stations selected for each state.

State	IL	IN	IA	KS	MI	MN	MO	NE	ND	OH	SD	WI
Station number	120	89	113	150	140	140	130	128	79	100	114	147

2.2.1. Input and output of APSIM simulation

The APSIM model simulates corn yield based on four weather data inputs: maximum and minimum temperature (Tmax and Tmin), precipitation (PPT), and radiation (Radn). The simulation also requires the station’s latitude, longitude, and year. Some management parameters are also necessary, including start and end of sowing window, plant population, fertilizer amount, and initial soil water, etc (Sec. 3.3.1). Tmax and Tmin influence the rate of plant development, and affect processes like photosynthesis and respiration. PPT are essential for modeling soil moisture levels, which directly affect water availability for crops. Radn is a critical factor in photosynthesis, as it provides the energy needed for plant growth. These weather data of IEM stations are available from the IEM website (Herzmann et al., 2004). The APSIM model takes weather data as input to simulate root zone soil moisture (SM_rootzone), surface soil moisture (SM_surface), and corn yield.

SM_rootzone is crucial for corn growth as it directly affects water availability for uptake, influencing plant development and yield. SM_surface plays a key role in seed germination and early growth stages.

2.2.2. Variables summary in field-level dataset for pretraining

We calculated a five-year historical average yield based on the simulated corn yield to establish a local baseline for model accuracy improvement. We also included the prediction year and location (longitude and latitude) of IEM stations in the field-level dataset. Because soil properties and topography vary across space and time, year and location can help the ML model capture this variation. Then we combined the weather data, simulated soil moisture and corn yield, along with other variables to construct the APSIM field-level dataset (Table 3).

Table 3: Summary of variables comprising the APSIM field-level dataset, including inputs and simulated outputs

Category	Variables
Weather data	Radn (MJ/m ²) (input)
	Tmax (°C) (input)
	Tmin (°C) (input)
	PPT (mm) (input)
Soil moisture	SM_surface (simulated)
	SM_rootzone (simulated)
Corn yield	Corn yield (t/ha) (simulated)
Others	Prediction year (input)
	Location (Latitude and longitude) (input)
	Historical average yield (t/ha) (simulated)

2.3. GEE county-level dataset

In this section, we introduce how to construct a county-level dataset for finetuning. Details of the studied counties are provided in [Table 4](#). This dataset includes all the variable types in the APSIM field-level dataset ([Table 3](#)), including weather, soil moisture, and other features, but from different sources. To enhance ML model performance with RS data, we also included four Vegetation Indices (VIs) from satellite imagery: Green Chlorophyll Index (GCI), Enhanced Vegetation Index (EVI), Normalized Difference Water Index (NDWI), and Normalized Difference Vegetation Index (NDVI).

Table 4: The average number of counties selected for each state in GEE county-level dataset.

State	IL	IN	IA	KS	MI	MN	MO	NE	ND	OH	SD	WI
County number	91	74	87	74	57	64	74	69	48	72	39	62

2.3.1. Vegetation indices

The Terra and Aqua combined Moderate Resolution Imaging Spectroradiometer (MODIS) Land Cover Climate Modeling Grid Version 6 data product (MCD12Q1 v6) ([Schaaf and Wang, 2015](#)) is a vital source of satellite-derived data with 500 m resolution, providing consistent, high-quality observations of the Earth’s surface. MODIS MCD12Q1 v6 captures data in multiple spectral bands and offers various products like VIs. These indices are essential for monitoring vegetation health, biomass, water content, and chlorophyll levels across different regions and time scales. They help improve yield prediction by indicating vegetation growth and crop health.

The Green Chlorophyll Index (GCI) ([Gitelson et al., 2005](#)) is used to estimate the chlorophyll content in plants, which directly relates to plant health

and productivity. It is calculated using the near-infrared (NIR) and green spectral bands. GCI is valuable for assessing vegetation health, especially for monitoring crop growth and detecting areas with nutrient deficiencies. High chlorophyll content typically indicates a healthy, productive plant, making GCI an essential tool in agricultural management. GCI is defined as:

$$GCI = \frac{NIR}{Green} - 1 \quad (1)$$

where *NIR* represents the surface reflectance in the Near Infrared band, and *Green* represents the surface reflectance in the Green band.

The Enhanced Vegetation Index (EVI) (Huete et al., 2002) is designed to optimize the vegetation signal by enhancing sensitivity in high biomass areas and reducing atmospheric and canopy background noise. It uses the red, blue, and NIR spectral bands. EVI is particularly useful in regions with dense vegetation, where NDVI might saturate. It provides a more accurate representation of vegetation conditions, especially in areas with high leaf area index, making it ideal for monitoring forests and agricultural lands. EVI is defined as:

$$EVI = 2.5 \times \frac{NIR - Red}{NIR + 6 \times Red - 7.5 \times Blue + 1} \quad (2)$$

where *Red* and *Blue* represent the surface reflectances of the Red band and Blue band, respectively.

The Normalized Difference Water Index (NDWI) (Gao, 1996) measures the

moisture content in vegetation and soil by using the NIR and shortwave infrared (SWIR) bands. NDWI is crucial for monitoring water stress in plants, assessing drought conditions, and detecting changes in water bodies. It aids in managing irrigation practices and understanding the impact of water availability on crop yields. NDWI is defined as:

$$NDWI = \frac{NIR - SWIR}{NIR + SWIR} \quad (3)$$

where *SWIR* represents the shortwave infrared band.

The Normalized Difference Vegetation Index (NDVI) ([KRIEGLER, 1969](#)) is one of the most widely used indices for measuring vegetation greenness and biomass. It is calculated using the NIR and red spectral bands. NDVI is a standard tool for monitoring plant growth, assessing vegetation cover, and detecting changes in biomass over time. It is particularly useful for tracking seasonal variations in vegetation and estimating crop yields. NDVI is defined as:

$$NDVI = \frac{NIR - RED}{NIR + RED} \quad (4)$$

2.3.2. Weather data

The Parameter-elevation Regressions on Independent Slopes Model (PRISM) dataset ([Daly et al., 2015](#))([Daly et al., 2008](#)) is a high-resolution weather dataset with 4 km resolution that provides detailed information on various climatic variables, including PPT, Tmax, and Tmin. This dataset is widely used in agricultural research, hydrology, and weather studies due to its fine

spatial resolution and comprehensive coverage, making it an essential tool for understanding and predicting weather-related impacts on crop yield and other environmental processes.

The MCD18A1 Version 6.1 (Wang, 2021) is a MODIS Terra and Aqua combined Downward Shortwave Radiation gridded Level 3 product. The reliable radiation data (Radn) is produced daily at 500 m resolution, with estimates of Downward Shortwave Radiation provided every 3 hours. Downward Shortwave Radiation is incident solar radiation over land surfaces in the shortwave spectrum (300-4,000 nanometers) and is an important variable in land-surface models that address a variety of scientific and applied issues.

2.3.3. Soil moisture

The SPL4SMGP.007 SMAP L4 Global 3-hourly 9-km Surface and Root Zone Soil Moisture dataset (Reichle et al., 2022) plays a critical role in our research on the relationship between drought and corn yield prediction. By providing detailed measurements of soil moisture at both the surface (0–5 cm) and root zone levels (0–100 cm), SMAP level 4 data allows us to assess the availability of water in the soil, a key factor influencing crop growth and resilience during drought conditions.

2.3.4. Variables summary in county-level dataset for finetuning

Additional features included the prediction year, location (latitude and longitude), and the 5-year historical average yield (USDA, 2020). These features were also added to the GEE county-level dataset, consistent with their inclusion in the APSIM field-level dataset. All the variables in GEE county-level dataset are listed in Table 5.

Table 5: Summary of variables in GEE county-level dataset

Category	Variables	Spatial resolution	Source
Vegetation index	Green Chlorophyll Index (GCI)	500m	MODIS
	Enhanced Vegetation Index (EVI)		
	Normalized Difference Water Index (NDWI)		
	Normalized Difference Vegetation Index (NDVI)		
Weather data	Radn (W/m^2)	4km	PRISM
	Tmax ($^{\circ}C$)		
	Tmin ($^{\circ}C$)		
	PPT (mm)		
Soil moisture	SM_surface	9km	SMAP
	SM_rootzone		
Corn yield	USDA NASS corn yield (t/ha)	N/A	USDA NASS
Others	Prediction year		
	Location (Latitude and longitude)		
	Historical average yield (t/ha)		

3. Methodology

The overall pipeline of the KGML-SM is shown in Fig. 2. This architecture comprised two principal components: the W2S encoder, designed to capture the relationship between weather data and soil moisture, and the attention-based feature-weighting module, which learned how various features influence corn yield. Initially, the model was pretrained on the APSIM field-level dataset, followed by finetuning using the GEE county-level dataset.

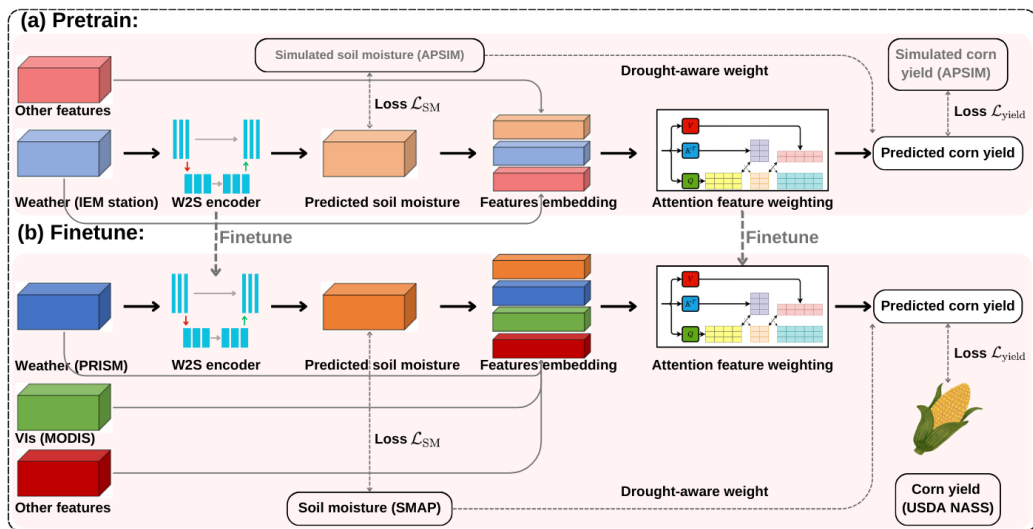


Figure 2: The pipeline of the proposed KGML-SM model.

We begin with a formal problem formulation of KGML-SM (Sec. 3.1), followed by an introduction to the model components (Sec. 3.2); next, we explain how the APSIM field-level dataset is generated for pretraining (Sec. 3.3) and the GEE county-level dataset for finetuning and testing (Sec. 3.4); finally, we introduce how the KGML-SM model is trained and used for prediction (Sec. 3.5).

3.1. Problem formulation

The corn yield prediction problem is formally defined in this section, along with its mathematical formulation within the KGML framework. Let each unique county-year combination be represented by a sample indexed as i ($i = 1, 2, \dots, N$), where N is the total number of county-year instances in the experiment. For each sample i , the input features are specified as follows: The temporal weather features are denoted by the vector $\mathbf{w}_i = [w_i^1, w_i^2, \dots, w_i^T]$. Other features, including the prediction year, geographical location, and historical average yield, are aggregated into the vector $\mathbf{o}_i = [o_i^1, o_i^2, \dots, o_i^T]$. In these representations, T corresponds to the total number of discrete time steps covering the duration from corn planting to harvest. Additionally, simulated soil moisture data is represented as $\mathbf{s}_i = [s_i^1, s_i^2, \dots, s_i^T]$. The corn yield record for sample i is denoted by y_i and serves as the supervision for model training.

The APSIM-generated field-level dataset, specified as $\mathcal{D}_{\text{field/pretrain}} = \{(\mathbf{w}_i, \mathbf{o}_i \mid \mathbf{s}_i, \mathbf{y}_i)\}$, is employed for the pretraining phase. In this notation, the vertical bar \mid separates the input variables $(\mathbf{w}_i, \mathbf{o}_i)$ from the target labels $(\mathbf{s}_i, \mathbf{y}_i)$. Furthermore, VIs represented by the vector $\mathbf{v}_i = [v_i^1, v_i^2, \dots, v_i^T]$ are incorporated.

The county-level dataset derived from GEE is denoted as $\mathcal{D}_{\text{county/finetune}} = \{(\mathbf{w}_i, \mathbf{o}_i, \mathbf{v}_i \mid \mathbf{s}_i, \mathbf{y}_i)\}$ and is utilized for the finetuning.

The objective is to first build the W2S encoder f_{W2S} to map weather inputs to soil moisture $\hat{\mathbf{s}}_i = f_{\text{W2S}}(\mathbf{w}_i)$. Then, the predicted soil moisture $\hat{\mathbf{s}}_i$ is combined with other input features to predict yield via an attention module f_{att} , resulting in the prediction $\hat{y}_i = f_{\text{att}}(\mathbf{w}_i, \mathbf{o}_i, \mathbf{v}_i, \hat{\mathbf{s}}_i)$. The model’s performance is evaluated by comparing the predicted yields \hat{y}_i with the actual yields y_i .

3.2. KGML-SM model structure

3.2.1. Weather-to-Soil encoder

The W2S encoder is a module designed to model the influence of weather conditions on soil moisture. By capturing the relationship between weather and soil moisture, the W2S encoder improves the model’s understanding of soil dynamics and the impact of weather variability on soil conditions and corn yield.

The W2S encoder employs a U-Net-based encoder-decoder architecture, which consists of an encoder, a decoder, and a fully connected layer (Goodfellow et al., 2016) for feature transformation. Given a time-series weather input \mathbf{w}_i , the encoder extracts hierarchical representations by progressively down-sampling the temporal dimension. The decoder then reconstructs high-level features using upsampling and skip connections that integrate information from the encoder. Finally, a fully connected layer transforms the decoded features into the predicted soil moisture output $\hat{\mathbf{s}}_i = f_{\text{W2S}}(\mathbf{w}_i)$.

3.2.2. Attention module

The attention mechanism (Vaswani, 2017) is a powerful tool in ML that enables models to focus on the most relevant parts of the input data when making predictions. By assigning different levels of importance to various input elements, the attention mechanism helps the model prioritize the most crucial information. In KGML-SM, we aim to use the attention mechanism to weight different features, helping us understand each feature’s contribution to yield prediction across different dimensions.

The input for corn yield prediction is formulated as $\mathbf{X}_i = [\mathbf{w}_i; \mathbf{o}_i; \mathbf{v}_i; \hat{\mathbf{s}}_i]$ representing the concatenation of feature vectors. For each feature embedding \mathbf{X}_i , an attention mechanism is employed to learn the corresponding attention weight α_i . This weight is subsequently utilized in the computation of the final yield \hat{y}_i .

First, we compute the query \mathbf{Q}_i , key \mathbf{K}_i , and value \mathbf{V}_i vectors from the feature \mathbf{X}_i using learned linear transformations:

$$\mathbf{Q}_i = \mathbf{W}_Q \mathbf{X}_i, \quad \mathbf{K}_i = \mathbf{W}_K \mathbf{X}_i, \quad \mathbf{V}_i = \mathbf{W}_V \mathbf{X}_i \quad (5)$$

where \mathbf{W}_Q , \mathbf{W}_K , and \mathbf{W}_V are the learned weight matrices for the query, key, and value, respectively.

Next, we calculate the attention scores by taking the dot product of the query and key, scaled by the square root of the key’s dimension d_k :

$$\text{Attention}(\mathbf{Q}_i, \mathbf{K}_i) = \frac{\mathbf{Q}_i \cdot \mathbf{K}_i^\top}{\sqrt{d_k}} \quad (6)$$

These attention scores are then passed through a softmax function (Goodfellow et al., 2016) to obtain the weights α_i :

$$\alpha_i = \text{softmax} \left(\frac{\mathbf{Q}_i \cdot \mathbf{K}_i^\top}{\sqrt{d_k}} \right) \quad (7)$$

The softmax function converts a vector of K real numbers into a probability distribution of K possible outcomes. Given a random input vector $\mathbf{z} = [z_1, \dots, z_K]$ for $i = 1, \dots, K$, the softmax function (Goodfellow et al., 2016) is defined as:

$$\text{softmax}(\mathbf{z})_i = \frac{e^{z_i}}{\sum_{j=1}^K e^{z_j}} \quad (8)$$

where e^{z_i} is the exponential of the i -th element of the input vector \mathbf{z} .

Finally, we compute the weighted sum of the values \mathbf{V}_i to obtain the final yield prediction:

$$\hat{y}_i = \sum_{t=1} \alpha_t \mathbf{V}_t \quad (9)$$

3.3. Generating APSIM field-level dataset for pretraining

The variables comprising the field-level dataset were previously introduced (Sec. 2.2); this section provides additional processing details. Besides the

input weather data obtained from IEM, specific management parameters were also necessary for model calibration (Sec. 3.3.1). Following the simulation, the resulting data required an optimizing process prior to its utilization (Sec. 3.3.2).

3.3.1. APSIM management parameters

Simulation methodology depends on the study's scale. For field-level areas, management information is obtained directly from farmers as input. Other unknown parameters are adjusted to optimize the model (Shahhosseini et al., 2021). For county-level areas, identifying representative fields is common practice. Their management parameters are averaged, and then applied to represent the entire county (Puntel et al., 2016). Calibrating each county individually became impractical for very large study areas like our U.S. Corn Belt simulation. In such cases, the typical approach defines a parameter range based on empirical and statistical data. These parameters are then randomly combined within specified ranges, simulating yield across all counties (Lobell et al., 2015). Given the vast area of cornfields in our study, it was not feasible to calibrate these parameters for every individual station. Therefore, we established a general parameter range encompassing all possible values across different fields. This approach ensured model applicability across a wide range of conditions, maintaining reasonable prediction accuracy.

Some reasonable adjustment ranges for key management parameters were collected from prior research and USDA statistics (Table 6). Sowing density determines the number of plants per unit area, directly affecting competition for resources such as light, water, and nutrients. Based on statistics from

the USDA NASS (USDA, 2020), the range for sowing density was set at 6-9 plants/m², values of 6,7,8, and 9 were used in the simulation. Sowing dates are crucial as they determine the crop’s growth cycle and its interaction with seasonal weather patterns. Typically, growers maximize corn yield by planting in late April or early May (Licht, 2021; Coulter, 2024). In the simulation, sowing started between April 20–25 and ended between May 15–20. Fertilizer application is essential for providing the necessary nutrients to support plant growth. The most commonly used nitrogen fertilizers for corn production in North America are anhydrous ammonia, urea, and urea-ammonium nitrate solutions (Herzmann et al., 2004). The fertilizer amount was set at 200-300 kg/ha of urea nitrogen (N), values of 200, 250, and 300 were used in the simulation. Initial soil water content is important for establishing the starting conditions for the model’s simulation of soil moisture dynamics throughout the growing season. The initial soil water content was set between 40% and 60%, values of 40%, 50%, and 60% were used in the simulation.

Table 6: Summary of management parameters in APSIM simulation

Factor	Value range	Source
Start of sowing window	Apr-20 to Apr-25	(Licht, 2021; Coulter, 2024)
End of sowing window	May-15 to May-20	(Licht, 2021; Coulter, 2024; Lobell et al., 2015)
Plant population	6-9 plants/m ²	(USDA, 2020)
Fertilizer amount	200-300 kg/ha	(Herzmann et al., 2004)
Initial soil water	40%-60%	(Lobell et al., 2015)

3.3.2. Optimizing APSIM field-level dataset based on soil moisture

APSIM is not accurate for large-scale corn yield simulation without precise management adjustments, thus requiring optimization of the APSIM field-level pretrain dataset. Soil moisture was proposed as a benchmark for filtering high-quality data. First, soil moisture dynamics are relatively simple, strongly correlated with precipitation. In contrast, corn yield is influenced by multiple factors and complex growth processes, hindering accurate modeling in process-based model. Second, simulation processes inherently exhibit cumulative error. Due to the relative simplicity of soil moisture modeling, this error is comparatively smaller. Therefore, the APSIM field-level dataset was optimized based on the quality of soil moisture data. Specifically, an LR model was trained on the GEE county-level dataset. It utilized four weather inputs (Tmax, Tmin, PPT, Radn) to predict soil moisture output. The trained model subsequently predicted soil moisture for the APSIM field-level dataset using its weather data. This prediction was compared against the simulated soil moisture. Simulated soil moisture with a mean squared error (MSE) exceeding 0.5 were discarded ensuring dataset quality.

3.4. Generating GEE county-level dataset for finetuning and testing

3.4.1. Feature Extraction Within Cornfield

To focus on the corn portion of the acquired feature data from GEE, the cornfield areas had to be identified. The Cropland Data Layer (CDL) cropland mask ([USDA-NASS, 2017](#)) was utilized extracting feature data corresponding to cropland. The Cropland Data Layer is an annual raster-based dataset. It provides crop-specific land cover information produced by the USDA. This dataset has a 30-meter resolution. The CDL was employed to generate a

cornfield mask in GEE, supporting our corn yield prediction study in twelve U.S. Corn Belt states.

3.4.2. Data preprocessing

County-level features were aggregated into a single value every 16 days, representing agricultural conditions for that period. This process resulted in a data vector for each feature annually for each county. This aggregation method followed the experimental setup from previous research (Ma et al., 2021b; Wang et al., 2025).

3.5. Developing the KGML-SM framework

3.5.1. Pretraining with APSIM field-level dataset

The pretraining process began by using a W2S encoder f_{W2S} to learn the relationship between input weather features \mathbf{w}_i and predicted soil moisture $\hat{\mathbf{s}}_i$. This process was formulated as $\hat{\mathbf{s}}_i = f_{W2S}(\mathbf{w}_i)$, where $\mathbf{w}_i \in \mathcal{D}_{\text{field/pretrain}}$. Then, The simulated soil moisture $\mathbf{s}_i \in \mathcal{D}_{\text{field/pretrain}}$ is used to guide the W2S encoder. The loss function \mathcal{L}_{SM} was defined as:

$$\mathcal{L}_{SM} = \frac{1}{N} \sum_{i=1}^N (\mathbf{s}_i - \hat{\mathbf{s}}_i)^2 \quad (10)$$

Next, the predicted soil moisture was concatenated with weather data and other features to form the features embedding $\mathbf{X}_i = [\mathbf{w}_i; \mathbf{o}_i; \hat{\mathbf{s}}_i]$. The final corn yield \hat{y}_i was predicted using the attention module f_{att} , with the concatenated features \mathbf{X}_i as input:

$$\hat{y}_i = f_{att}(\mathbf{X}_i) \quad (11)$$

3.5.2. Drought-aware yield prediction loss function

Soil moisture is widely recognized to affect crop yield (Ines et al., 2013; Bushong et al., 2016) and numerous studies explored this relationship (Mladenova et al., 2017; Vergopolan et al., 2021; Pignotti et al., 2023). However most prior studies lacked an elegant quantitative approach addressing this issue. This study introduces a loss function adjusting predicted corn yield based on varying soil moisture levels.

The final yield prediction loss function was designed to improve the model’s accuracy while incorporating drought sensitivity and penalizing overestimation. It was formulated as:

$$\mathcal{L}_{\text{yield}} = \frac{1}{N} \sum_{i=1}^N d_i [(y_i - \hat{y}_i)^2 + \lambda \max(0, \hat{y}_i - y_i)^2] \quad (12)$$

where d_i is a drought-aware weighting factor, which was defined as:

$$d_i = \frac{1}{\bar{s}_i + \varepsilon} \quad (13)$$

where \bar{s}_i is the average soil moisture over the growing season for sample i , and ε is a small constant to prevent numerical instability. We set $\varepsilon = 1$ in our experiment. Since soil moisture plays a critical role in crop growth and yield formation, the loss function assigned a higher penalty to drier conditions, encouraging the model to be more responsive to soil moisture variations.

Additionally, there is an asymmetric penalty term (Ridnik et al., 2021) controlled by the factor $\lambda > 0$, which amplifies the loss when the predicted yield

\hat{y}_i exceeds the true yield y_i :

$$\lambda \max(0, \hat{y}_i - y_i)^2 \tag{14}$$

This asymmetry discourages overestimation, particularly under drought conditions, where yield predictions tend to be more uncertain. By applying a stronger penalty to overestimated yields, the model is encouraged to be more conservative, reducing the risk of unrealistic predictions. We set $\lambda = 2$ in our experiment.

Specifically, when $\hat{y}_i > y_i$, the predicted error is scaled by a penalty factor λ , amplifying the loss in these cases. This encourages the model to adopt a conservative approach, reducing the likelihood of overestimating yield, particularly in drought-prone regions where overestimation could lead to inaccurate agricultural planning.

This whole loss function formulation ensured that the model not only learned accurate yield predictions but also captured the impact of soil moisture variability and drought stress, leading to more reliable and interpretable results.

3.5.3. Finetuning and testing with GEE county-level dataset

Following the pretraining of the model on the APSIM field-level dataset $\mathcal{D}_{\text{field/pretrain}}$, finetuning using the GEE county-level dataset $\mathcal{D}_{\text{county/finetune}}$ was required to improve the model for the county-level corn yield prediction task. This process involved initially partitioning the data into training, validation, and test sets, followed by predicting corn yield for the target years. Specific details regarding the partition and utilization of these datasets are elaborated

upon in the experimental setup (Sec. 4.1). The loss functions $\mathcal{L}_{\text{yield}}$ and \mathcal{L}_{SM} were also optimized on the training and validation datasets.

4. Experimental Results

4.1. Experimental setup

We conducted experiments on both traditional ML models and DL models. When predicting corn yield for a specific year, we trained the model using all data from preceding years, then split the dataset into 80% for training and 20% for validation, and tested it on the target year. Each experiment was conducted five times with different random seeds, and the final results represented the average across these runs to ensure robustness and reliability.

We implemented the DL models using the PyTorch framework (Paszke et al., 2019) and the traditional ML code with sklearn (Pedregosa et al., 2011). The models were run on A100-SXM4-40GB and A100-SXM4-80GB GPUs. For training, we used the ADAM optimizer (Kingma and Ba, 2014) with an initial learning rate of 0.001 and the ReduceLROnPlateau scheduler.

Root mean square error ($RMSE$) and the coefficient of determination (R^2) were used to evaluate the performance of our model. The formulas for $RMSE$ and R^2 are:

$$RMSE = \sqrt{\frac{1}{n} \sum_{i=1}^n (y_i - \hat{y}_i)^2} \quad (15)$$

$$R^2 = 1 - \frac{\sum_{i=1}^n (y_i - \hat{y}_i)^2}{\sum_{i=1}^n (y_i - \bar{y})^2} \quad (16)$$

where n is the number of observations, y_i is the actual value for the i -th observation, \hat{y}_i is the predicted value for the i -th observation, and \bar{y} is the mean of the actual values.

4.2. Statistical analysis of drought, soil moisture, and corn yield

To study the impact of soil moisture on corn yield in the KGML-SM model and provide interpretability, we first analyzed the statistics of drought, soil moisture, and corn yield. The analysis aims to determine which regions experienced drought and reduced corn yield, and their relationship with soil moisture.

4.2.1. Specifying drought area

We investigated drought conditions in the United States ([Drought.gov](https://www.drought.gov), 2024) during the corn growth season (June-September) ([USDA](https://www.usda.gov), 2025) from 2019 to 2023 and present the corresponding maps ([Fig. 3](#)). In 2019 ([Fig. 3\(a\)](#)), drought conditions were predominantly observed in Iowa and Michigan. By 2020 ([Fig. 3\(b\)](#)), Iowa experienced severe drought, while moderate conditions affected North Dakota, South Dakota, Nebraska, and Illinois. Conditions deteriorated further in 2021 ([Fig. 3\(c\)](#)), with severe drought covering large parts of North Dakota, South Dakota, and Minnesota, while Nebraska and Iowa experienced moderate drought. In 2022 ([Fig. 3\(d\)](#)), severe drought persisted in Nebraska and Kansas, with South Dakota and Iowa experiencing moderate drought. In 2023 ([Fig. 3\(e\)](#)), severe drought was widespread across Nebraska, Kansas, Minnesota, Iowa, and Wisconsin, while Missouri faced moderate drought conditions.

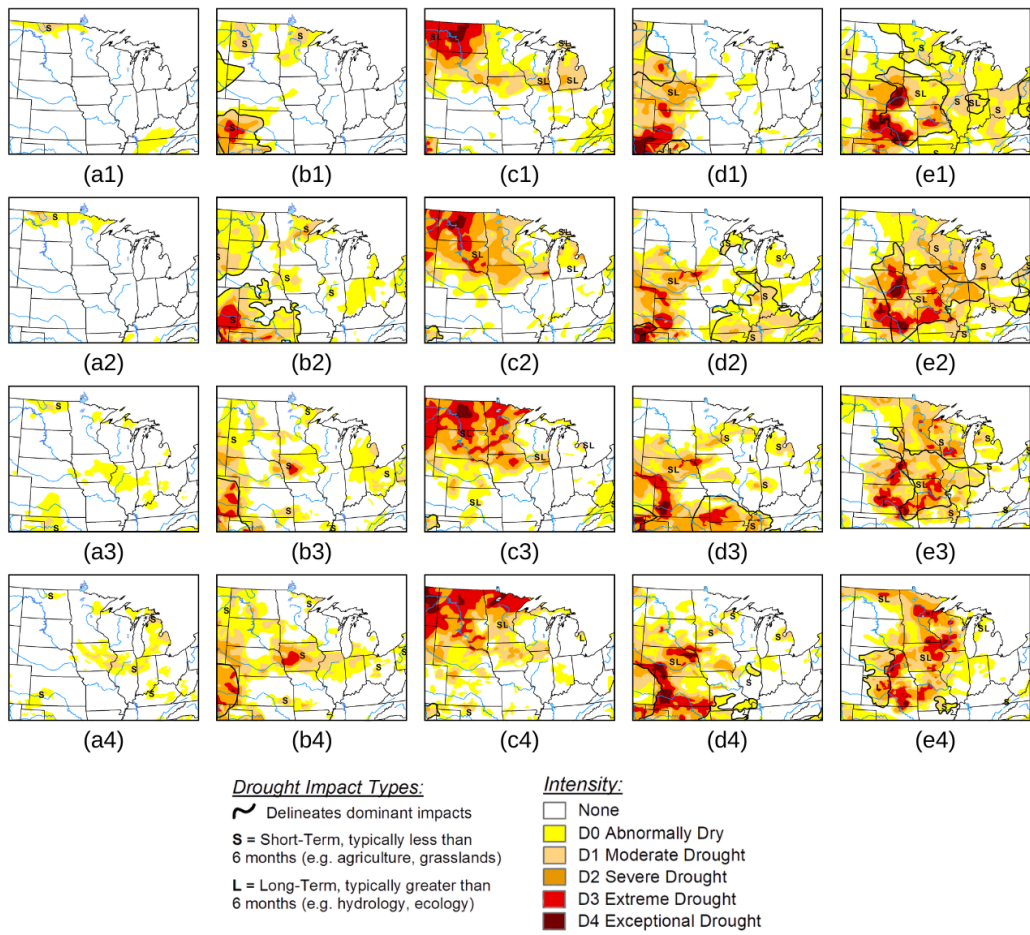


Figure 3: Drought map of the U.S. for (1) June - (4) September from (a) 2019 to (e) 2023.

4.2.2. Soil moisture statistics

Next, we specified the relationship between soil moisture and drought. Fig. 4 shows the maps of average rootzone and surface soil moisture during June-September from 2019 to 2023. The comparison of the drought maps above with soil moisture data from 2019 to 2023 revealed a strong correlation between drought-affected areas and lower soil moisture levels. We also noticed that rootzone moisture was more abundant than surface moisture and that the two spatial distributions were generally similar.

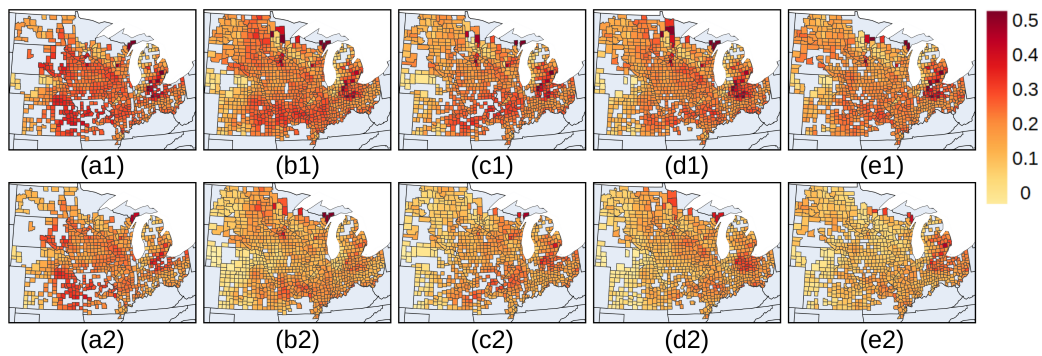


Figure 4: This figure shows the maps of average (1) rootzone and (2) surface soil moisture during June-September from (a) 2019 to (e) 2023.

4.2.3. Drought impact on corn yield

Finally, we examined the specific impact of drought on corn yield. We plotted the difference in corn yield for each year from 2019 to 2023 relative to the previous year's yield (Fig. 5), where negative values indicate a yield reduction. In 2019 (Fig. 5(a)), drought-affected areas included Iowa and Michigan; however, significant yield reductions were observed only in Michigan. In 2020 (Fig. 5(b)), Iowa faced drought along with a derecho storm (Hosseini et al., 2020), leading to noticeable yield losses. In 2021 (Fig. 5(c)), drought impacted North Dakota, South Dakota, Minnesota, Nebraska, and Iowa, yet significant yield reductions occurred only in North Dakota and South Dakota. In 2022 (Fig. 5(d)), drought-affected states included Nebraska, Kansas, South Dakota, and Iowa, but yield declines were primarily observed in Nebraska, Kansas, and South Dakota. In 2023 (Fig. 5(e)), although Nebraska and Kansas continued to experience drought, corn yield did not decrease significantly compared to the previous year, likely due to the already reduced yield in 2022. However, Iowa and Missouri experienced some yield losses due to ongoing drought conditions. Thus, we concluded that drought consistently led to a decline in corn yield.

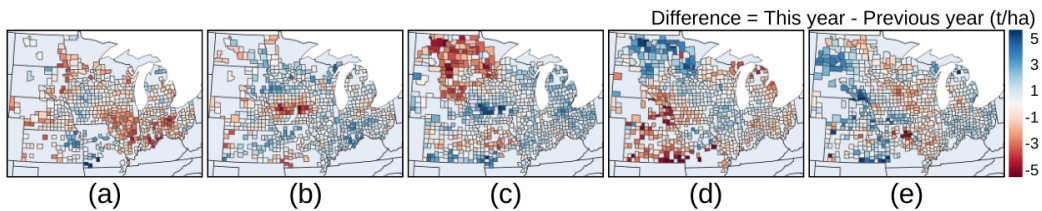


Figure 5: The difference in corn yield between each year from (a) 2019 to (e) 2023 and the previous year, with negative values indicating a reduction in yield.

4.2.4. Statistical summary of drought-affected states

Based on the above statistical analysis, we summarized the drought-affected areas that experienced yield reductions in [Table 7](#). In the experiment, we focused on these states that were affected by drought and experienced yield reductions.

Table 7: Summary of obviously yield-reduced states within drought-affected areas.

Year	Area type	Drought-affected states	Obviously yield-reduced states
2019		IA,MI	MI
2020		IA,ND,SD,NE,IL	IA
2021		ND,SD,MN,NE,IA	ND,SD
2022		NE,KS,SD,IA	NE,KS,SD
2023		NE,KS,MN,IA,WI,MO	IA,MO

4.3. Evaluation results

To validate the superiority of our KGML-SM model, we compared it with some commonly used ML models in remote sensing: LR, multilayer perceptron (MLP), ridge regression (RR), and random forest (RF). LR (Bishop and Nasrabadi, 2006) is a simple statistical method that models the relationship between a dependent variable and one or more independent variables by fitting a linear equation to the data. MLP (Goodfellow et al., 2016) is a neural network with multiple layers, including an input, hidden, and output layer. It captures non-linear relationships and is widely used for classification and regression. RR (Hoerl and Kennard, 1970) is an extension of linear regression that includes an L2 regularization term to prevent overfitting by penalizing large coefficients. RF (Breiman, 2001) is an ensemble learning method that constructs multiple decision trees during training and aggregates their predictions to improve accuracy and robustness.

The results showed that our KGML-SM model consistently outperformed other ML models across all years. As shown in Table 8, RF performed the best among traditional ML models, indicating its strong ability to capture complex relationships in the data (Couronné et al., 2018). RR performed slightly worse than RF, with slightly higher RMSE values, suggesting that regularization helped improve predictions but was not as effective as ensemble learning (Schreiber-Gregory, 2018). LR ranked next, showing higher RMSE values, likely due to its inability to model non-linear relationships effectively (Manual, 2013). MLP performed the worst, with the highest RMSE values in most years, indicating that it struggled to generalize well, possibly due to overfitting or insufficient training data (Caruana et al., 2000).

Table 8: Comparison with traditional ML models

Year	Method	KGML-SM		LR		MLP		RR		RF	
		RMSE	R2	RMSE	R2	RMSE	R2	RMSE	R2	RMSE	R2
2019		0.964	0.741	1.328	0.621	1.169	0.607	1.214	0.607	1.040	0.712
2020		0.980	0.792	1.304	0.690	1.207	0.734	1.230	0.661	1.120	0.719
2021		1.104	0.836	1.167	0.790	1.247	0.761	1.129	0.808	1.236	0.794
2022		1.085	0.837	1.471	0.740	1.400	0.765	1.318	0.781	1.185	0.821
2023		1.071	0.807	1.226	0.737	1.225	0.738	1.140	0.776	1.196	0.791

4.4. Ablation study of different components in KGML-SM model

To further demonstrate the contribution of each module in our KGML-SM model, we conducted a series of ablation studies. We began with a baseline model trained using only the GEE county-level dataset and the attention module (Att) (Wang et al., 2025). Next, we incorporated the APSIM field-level dataset pretraining to evaluate its impact on model performance (Att+sim). We then introduced the W2S encoder to assess its effectiveness in integrating soil moisture information (Att+sim+W2S). Finally, the impact of the drought-aware loss function was evaluated by comparing the performance of the KGML-SM model with the (Att+sim+W2S) model. We specifically compared the differences among models and their components in Table 9.

Table 9: Comparison of different methods and their components.

Method	Attention module	Field-level data pretraining	W2S encoder	Drought-aware loss
Att	✓			
Att+sim	✓	✓		
Att+sim+W2S	✓	✓	✓	
KGML-SM	✓	✓	✓	✓

Through the ablation study of all model components (Table 10), we found that the APSIM field-level dataset pretraining contributed the most to performance improvement. This indicated that our APSIM field-level dataset effectively captured county-level data patterns, playing a crucial role in enabling the model to learn the relationship between corn yield and agricultural variables. Additionally, our drought-aware loss function significantly enhanced performance in most years, demonstrating that incorporating prior knowledge of the relationship between drought and corn yield can effectively guide the training and prediction of ML models.

Table 10: Ablation study of different components in KGML-SM model

Year	Method		KGML-SM		Att+sim+W2S		Att+sim		Att	
	RMSE	R2	RMSE	R2	RMSE	R2	RMSE	R2	RMSE	R2
2019	0.964	0.741	0.974	0.732	1.087	0.715	1.268	0.57		
2020	0.98	0.792	0.981	0.783	1.003	0.77	1.011	0.77		
2021	1.104	0.836	1.127	0.811	1.143	0.814	1.195	0.808		
2022	1.085	0.837	1.119	0.802	1.144	0.802	1.315	0.779		
2023	1.071	0.807	1.101	0.805	1.114	0.781	1.201	0.766		

4.5. Spatial Visualization of model performance

In [Fig. 6](#), we plotted the error maps of the prediction results from 2019 to 2023 for the two best performed models: KGML-SM and RF model. In 2019 ([Fig. 6\(a\)](#)), the lower part of Michigan showed noticeable overestimation in the RF model, whereas our KGML-SM model performed well. In 2020 ([Fig. 6\(b\)](#)), although the derecho storm ([Hosseini et al., 2020](#)) in Iowa also had some impact on our KGML-SM model, we found that the RF model exhibited more severe overestimation. In 2021 ([Fig. 6\(c\)](#)), overestimation in the upper-left region, particularly in North Dakota and South Dakota, was significantly reduced. In 2022 ([Fig. 6\(d\)](#)), overestimation decreases notably in North Dakota, South Dakota, and Kansas, though the effect in Kansas was less pronounced. In 2023 ([Fig. 6\(e\)](#)), Iowa showed a reduction in overestimation, while the effect in Missouri was less noticeable. Overall, our model shows a notable improvement in addressing the issue of overestimation in drought-affected areas.

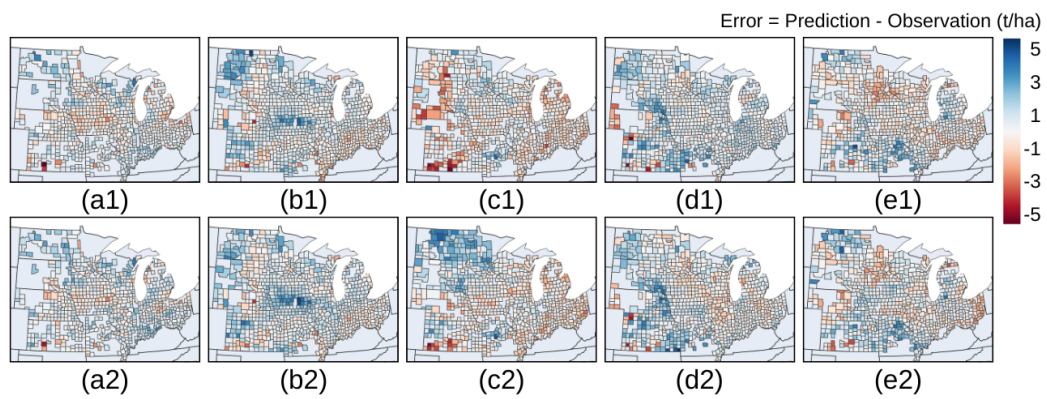


Figure 6: The error map for (1) KGML-SM and (2) RF model from (a) 2019 to (e) 2023, with blue indicating overestimation.

4.6. Understanding model bias and prediction-observation alignment

To analyze model prediction performance, we generated scatter plots for the KGML-SM model and the RF model (Fig. 7). These plots helped visualize the relationship between observed and predicted values, revealing patterns of overestimation, underestimation, and potential prediction biases across different years. In 2019 (Fig. 7(a)), the KGML-SM model presented a noticeably narrower distribution, indicating a lower spread in prediction errors. In 2020 (Fig. 7(b)), the predictions of the KGML-SM model were noticeably more concentrated along the diagonal and exhibited symmetry on both sides, whereas the RF model produced more dispersed predictions in high-yield regions. In 2021 (Fig. 7(c)), the RF model exhibited prediction collapse, where certain observed values correspond to nearly identical predicted values, likely due to overfitting or insufficient variability in learned representations. In 2022 (Fig. 7(d)) and 2023 (Fig. 7(e)), the KGML-SM model maintained a narrower and more concentrated prediction distribution. This comparison highlighted the advantage of the KGML-SM model in mitigating prediction collapse and improving overall robustness across different years.

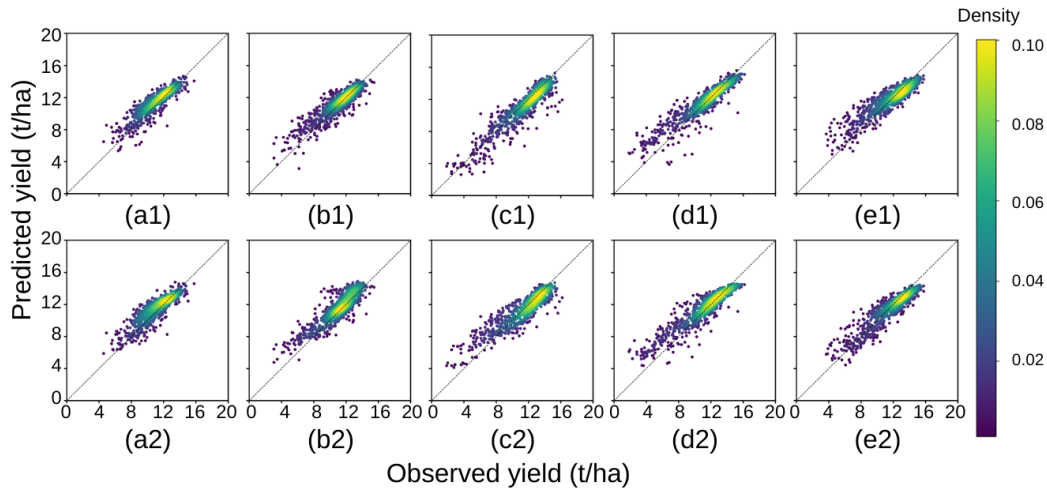


Figure 7: The scatter plot for (1) KGML-SM and (2) RF model from (a) 2019 to (e) 2023.

5. Discussion

In this section, we explore the role of soil moisture in model prediction from four questions:

- (Sec. 5.1) How did soil moisture influence model prediction spatially?
- (Sec. 5.2) How did soil moisture affect model performance throughout the corn growth season?
- (Sec. 5.3) how did soil moisture contribute to model prediction in drought and non-drought regions?
- (Sec. 5.4) How to interpret the observed inaccuracies in corn yield predictions based on soil moisture?

5.1. Spatial influence of soil moisture on model prediction

To answer the first question, we visualized the attention scores of soil moisture across twelve states in the U.S. Corn Belt from June to August over the years 2019 to 2023 (Fig. 8). The attention scores indicated the relative importance assigned to soil moisture by the model in different regions, with higher scores suggesting a stronger influence on yield prediction. The attention map highlighted how the model's reliance on soil moisture varied across different growth stages and drought conditions, allowing us to assess whether soil moisture has a greater impact on the model in drought-affected areas. To enhance visualization, we normalized attention values within each year. Consequently, analysis should focus on attention trends across regions within the same year rather than comparing values across different years.

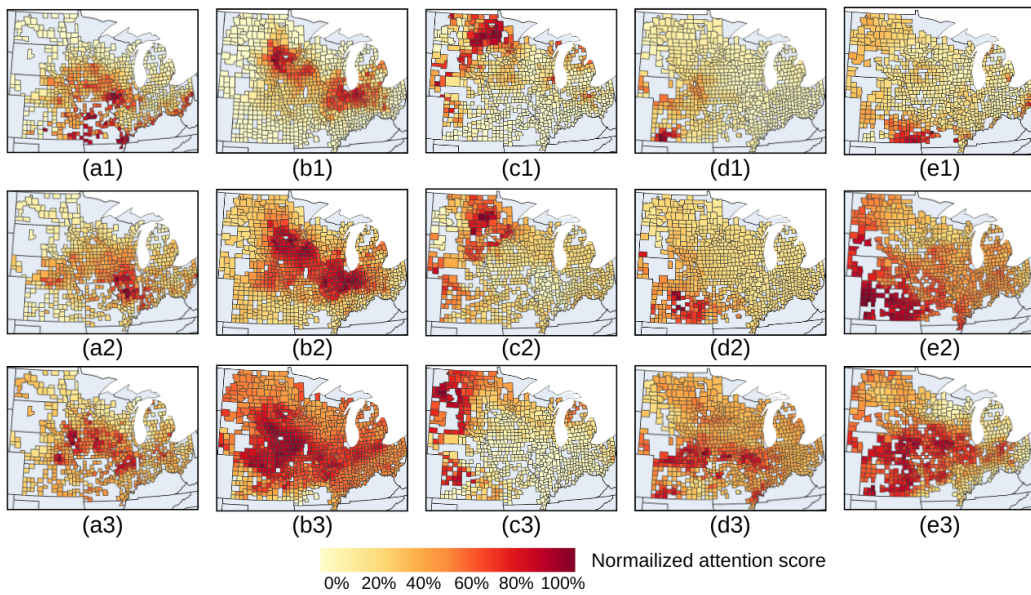


Figure 8: The attention visualization of soil moisture on corn yield prediction in different regions. The corn growth period was segmented into three stages, covering (1) June to (3) August, for the years (a) 2019 to (e) 2023. The attention visualization was computed by first calculating the attention values for all counties. These values were then normalized based on the maximum value in this year to ensure a consistent color scale, making the distribution more visually interpretable.

In June, during the early growth period, the attention scores for soil moisture were generally lower across all five years, This might be because the temperature was not too high and drought conditions were not severe at this time, leading to a less pronounced correlation between soil moisture and corn yield. In July, attention scores increased, particularly in drought-affected areas, as soil moisture became more influential during active growth and vegetative stages. By August, attention scores peaked in drought-affected states, aligning with the critical reproductive phase of corn when adequate soil moisture was essential for kernel development.

From 2019 to 2023, the attention distribution of soil moisture in corn yield prediction exhibited noticeable variations, aligning with the drought severity in different years. In early 2019 (Fig. 8(a1)), attention concentrated in Iowa. Subsequently (Fig. 8(a3)), regions with higher attention values expanded gradually, though Iowa retained the highest attention, aligning with observed drought conditions that year. During 2020 (Fig. 8(b)), high-attention regions were initially concentrated in Iowa and Nebraska, later expanding to adjacent areas. By 2021 (Fig. 8(c)), attention intensified over North Dakota, South Dakota, Minnesota, and Nebraska. In 2022 (Fig. 8(d)), high-attention areas were primarily located in Nebraska, Kansas, South Dakota, and Iowa. In 2023 (Fig. 8(e1)), attention initially focused on Kansas, expanding thereafter across a majority of states. Ultimately, significant attention emerged in Nebraska, Kansas, Minnesota, Iowa, Wisconsin, and Missouri, indicative of substantial drought conditions (Fig. 8(e3)). Overall, the period from 2019 to 2023 exhibited a trend of drought conditions and corresponding attention expanding towards the central United States, consistent with actual obser-

vations. The reason for the incomplete consistency between the two could be that although drought was present in the region, it did not severely impact corn yield. Alternatively, even without drought in a particular area, other factors, such as the derecho storm, might have affected corn yield. This analysis underscored the dynamic role of soil moisture in model prediction, with its importance intensifying during key growth stages and under severe drought conditions.

5.2. Temporal role of soil moisture during the corn growth season

To answer the second question and illustrate the impact of soil moisture at different stages of the corn growing season, we visualized the attention of three feature types—VIs, weather, and soil moisture—every 16 days from June to September in drought-affected states (Fig. 9). We found that the VIs had the highest influence on the model around August, which aligned with findings from previous study (Johnson, 2014). In this period, VIs showed the strongest correlation with corn yield because this period corresponded to the vegetative and reproductive growth stages, during which crop health and biomass accumulation significantly impact final yield (Huang et al., 2014). High VIs in this timeframe indicate optimal chlorophyll content, canopy development, and water availability, which are critical for photosynthesis and grain formation (Wang et al., 2005). Additionally, we found that weather data showed a significant increase in attention around July in 2020 (Fig. 9(b)) and 2022 (Fig. 9(d)), and the periods with noticeable attention spikes aligned with the trends of VIs. This phenomenon was more pronounced in soil moisture, as soil moisture attention showed a strong correlation with VIs in all years except 2022. In 2022, a slight increase in soil moisture attention could

still be observed near the VIs peak. This might be because VIs during these periods are closely related to certain weather data and soil moisture data. For example, NDWI increases with higher PPT because more rainfall enhances soil moisture and plant water content ([Ashok et al., 2021](#)). This indicated that our attention mechanism effectively captured feature importance over time dimension.

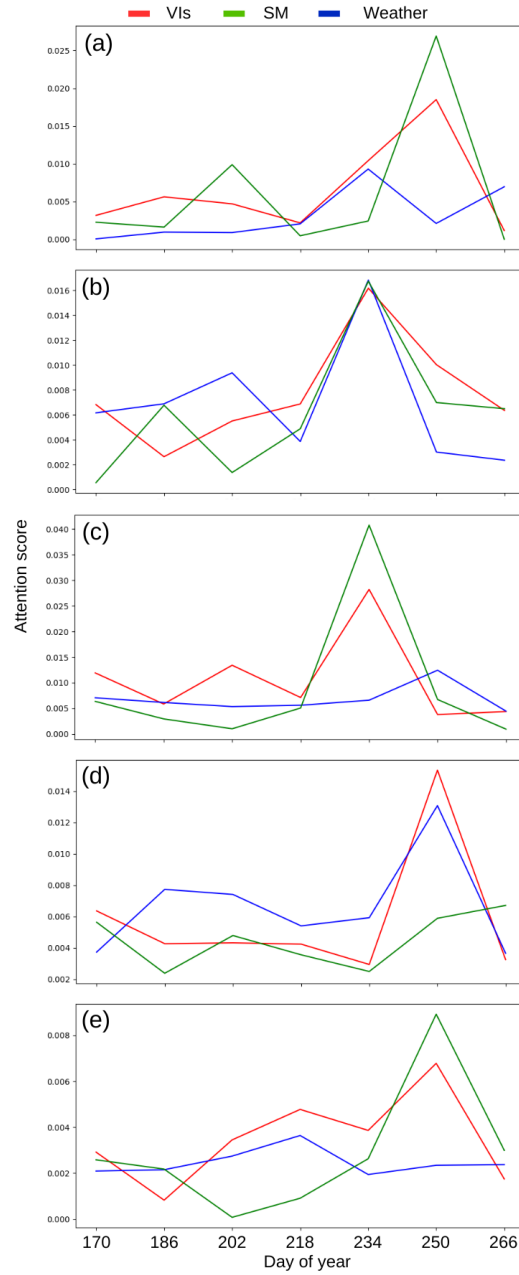


Figure 9: 5 year attention values of different feature types in the time series. The attention visualization is computed by first calculating the attention values for all features across all time points. Then, for each time point, we average the attention values across all features within the same category (VIs, Weather, and SM).

5.3. Statistical impact of soil moisture in drought and non-drought regions

To answer the third question, The box plot was used to illustrate the distribution of soil moisture attention across all counties from 2019 to 2023 (Fig. 10). Each point in this box plot represents a county, displaying the comparison of attention between red-marked drought-affected areas and blue-marked non-drought areas from 2019 to 2023 based on Table 7. Across all five years of attention values, drought-affected areas exhibited fewer outliers compared to non-drought areas, suggesting that the model's attention to soil moisture is more stable in drought-affected regions. Additionally, in all years, the median of soil moisture attention in drought-affected areas was consistently higher than in non-drought areas, indicating that soil moisture had a greater impact on the model in these areas.

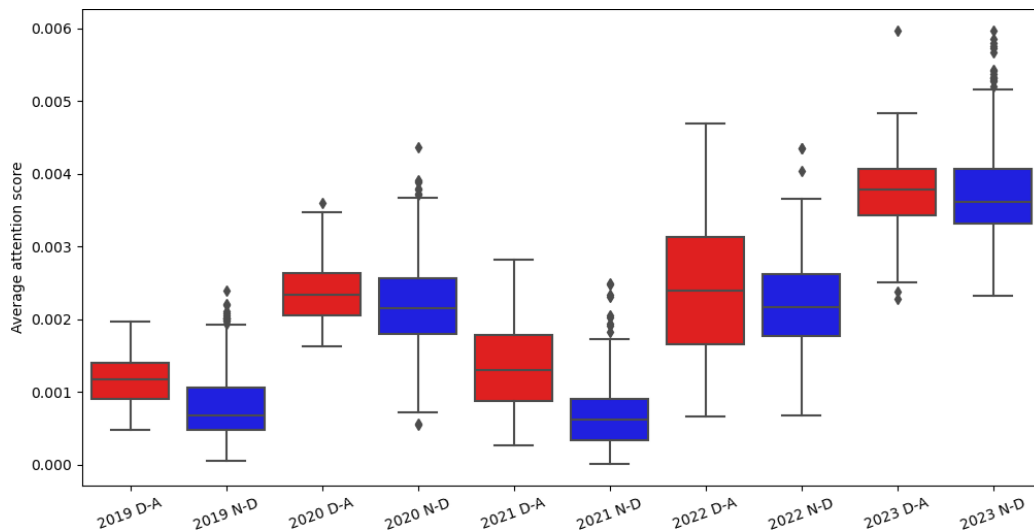


Figure 10: The boxplot of soil moisture attention in drought-affected areas (D–A) and non-drought areas (N–D) across all counties.

5.4. Interpreting corn yield prediction errors via soil moisture prediction anomalies

To answer the fourth question, we plotted the absolute error map of both soil moisture and corn yield predictions (Fig. 11). In our modeling process, we treated soil moisture as an intermediate variable to guide the corn yield output, so when corn yield prediction was inaccurate, the corresponding soil moisture might also exhibit anomalies. This analysis aims to conduct interpretability analysis of inaccurate corn yield predictions. In 2019 (Fig. 11(a)), the drought-affected state Michigan exhibited relatively accurate corn yield predictions from the KGML-SM model; however, the soil moisture output was less accurate. This suggested that soil moisture was challenging to predict in drought-affected areas. In 2020 (Fig. 11(b)), inaccurate corn yield prediction in Iowa was primarily attributable to the derecho storm’s impact (Hosseini et al., 2020), which soil moisture could not reflect. In 2021

(Fig. 11(c)), drought in North and South Dakota resulted in inaccurate corn yield predictions, and corresponding soil moisture predictions were also found to be inaccurate. In 2022 (Fig. 11(d)), Nebraska, Kansas, and South Dakota experienced drought, and their soil moisture predictions were also inaccurate. In 2023 (Fig. 11(e)), Iowa and Missouri were affected by drought. Iowa's corn yield and soil moisture prediction were accurate, which indicated that our model performed well. But the prediction for Missouri exhibited errors, despite relatively accurate corresponding soil moisture predictions for the state. According to report (Ward, 2023), some damaging winds and hail significantly impacted corn field, causing root lodging in late June and early July, particularly around Mooresville and Rockport, Missouri. Hail damage was also reported at Garden City, Missouri. These types of mechanical damage were not reflected in standard soil moisture data and constituted yield-limiting factors likely contributing to the corn yield prediction inaccuracies in Missouri. The analysis indicates that a significant portion of the error in corn yield prediction is related to soil moisture prediction error, given the key role soil moisture plays in corn growth; thus, if soil moisture is not accurately predicted, the accumulated error in modeling will lead to inaccurate corn yield prediction.

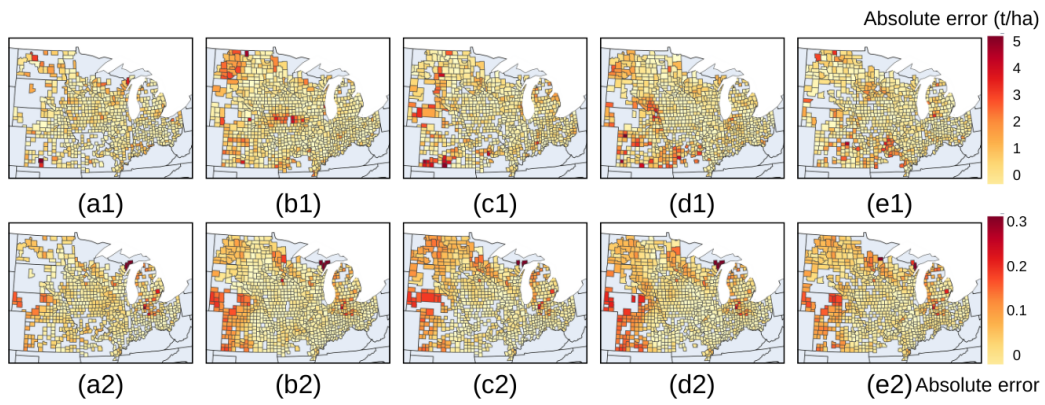


Figure 11: The absolute error map for (1) corn yield prediction and (2) soil moisture prediction from (a) 2019 to (e) 2023.

6. Conclusion

In this study, we proposed the KGML-SM model, where the W2S encoder is designed to capture the influence of weather on soil moisture, and the attention module is employed to weight different input features for final corn yield prediction. To address the known issue that drought conditions often lead to yield overestimation, we introduced a drought-aware loss function to mitigate this problem in drought-affected regions. We constructed both an APSIM field-level dataset and a GEE county-level dataset, leveraging a process-based model to learn the corn growth process by pretraining the KGML-SM model on the APSIM field-level dataset and finetuning it on the GEE county-level dataset. Our analysis covered 12 states in the U.S. Corn Belt to investigate the impact of soil moisture on corn yield prediction. The proposed method consistently outperformed baseline models across multiple test years. Furthermore, we studied the spatial and temporal influence of soil moisture through attention visualization, revealing when and where the model places greater focus on soil moisture. Finally, based on the relationship between soil moisture and corn yield prediction, we investigated the causes of inaccuracies in corn yield prediction and provided an explanation. In future work, we aim to apply transfer learning techniques to adapt models trained on well-studied regions with abundant simulated data to regions with limited data availability.

Funding

This work was supported by the United States Department of Agriculture (USDA) National Institute of Food and Agriculture (NIFA) Agriculture and

Food Research Initiative Foundational Program (Award No. 2022-67021-36468); and the USDA NIFA Hatch Project (Accession No. 7005141).

References

- Ashok, A., Rani, H.P., Jayakumar, K., 2021. Monitoring of dynamic wetland changes using ndvi and ndwi based landsat imagery. *Remote Sensing Applications: Society and Environment* 23, 100547.
- Bao, T., Jia, X., Zwart, J., Sadler, J., Appling, A., Oliver, S., Johnson, T.T., 2021. Partial differential equation driven dynamic graph networks for predicting stream water temperature, in: *2021 IEEE International Conference on Data Mining (ICDM)*, IEEE. pp. 11–20.
- Bishop, C.M., Nasrabadi, N.M., 2006. *Pattern recognition and machine learning*. volume 4. Springer.
- Breiman, L., 2001. Random forests. *Machine learning* 45, 5–32.
- Burroughs, C.H., Montes, C.M., Moller, C.A., Mitchell, N.G., Michael, A.M., Peng, B., Kimm, H., Pederson, T.L., Lipka, A.E., Bernacchi, C.J., et al., 2023. Reductions in leaf area index, pod production, seed size, and harvest index drive yield loss to high temperatures in soybean. *Journal of experimental botany* 74, 1629–1641.
- Bushong, J.T., Mullock, J.L., Miller, E.C., Raun, W.R., Klatt, A.R., Arnall, D.B., 2016. Development of an in-season estimate of yield potential utilizing optical crop sensors and soil moisture data for winter wheat. *Precision Agriculture* 17, 451–469.
- Caruana, R., Lawrence, S., Giles, C., 2000. Overfitting in neural nets: Back-propagation, conjugate gradient, and early stopping. *Advances in neural information processing systems* 13.

- Chen, S., Kalanat, N., Xie, Y., Li, S., Zwart, J.A., Sadler, J.M., Appling, A.P., Oliver, S.K., Read, J.S., Jia, X., 2023. Physics-guided machine learning from simulated data with different physical parameters. *Knowledge and Information Systems* 65, 3223–3250.
- Cooper, M., Gho, C., Leafgren, R., Tang, T., Messina, C., 2014. Breeding drought-tolerant maize hybrids for the us corn-belt: discovery to product. *Journal of Experimental Botany* 65, 6191–6204.
- Coulter, J., 2024. Planting date considerations for corn. <https://crops.extension.iastate.edu/blog/mark-licht-zachary-clemens/corn-and-soybean-planting-date-considerations>.
- Couronné, R., Probst, P., Boulesteix, A.L., 2018. Random forest versus logistic regression: a large-scale benchmark experiment. *BMC bioinformatics* 19, 1–14.
- Daly, C., Halbleib, M., Smith, J.I., Gibson, W.P., Doggett, M.K., Taylor, G.H., Curtis, J., Pasteris, P.P., 2008. Physiographically sensitive mapping of climatological temperature and precipitation across the conterminous united states. *International Journal of Climatology: a Journal of the Royal Meteorological Society* 28, 2031–2064.
- Daly, C., Smith, J.I., Olson, K.V., 2015. Mapping atmospheric moisture climatologies across the conterminous united states. *PloS one* 10, e0141140.
- Daw, A., Karpatne, A., Watkins, W.D., Read, J.S., Kumar, V., 2022. Physics-guided neural networks (pgnn): An application in lake temper-

- ature modeling, in: Knowledge Guided Machine Learning. Chapman and Hall/CRC, pp. 353–372.
- Drought.gov, 2024. U.s. drought monitor. <https://www.drought.gov/states/>.
- Dugdale, S.J., Hannah, D.M., Malcolm, I.A., 2017. River temperature modelling: A review of process-based approaches and future directions. *Earth-Science Reviews* 175, 97–113.
- Gao, B.C., 1996. Ndw— a normalized difference water index for remote sensing of vegetation liquid water from space. *Remote sensing of environment* 58, 257–266.
- Gitelson, A.A., Viña, A., Ciganda, V., Rundquist, D.C., Arkebauer, T.J., 2005. Remote estimation of canopy chlorophyll content in crops. *Geophysical research letters* 32.
- Goodfellow, I., Bengio, Y., Courville, A., 2016. Deep learning. MIT press.
- Gorelick, N., Hancher, M., Dixon, M., Ilyushchenko, S., Thau, D., Moore, R., 2017. Google earth engine: Planetary-scale geospatial analysis for everyone. *Remote Sensing of Environment* URL: <https://doi.org/10.1016/j.rse.2017.06.031>, doi:10.1016/j.rse.2017.06.031.
- Graham, R.L., Nelson, R., Sheehan, J., Perlack, R.D., Wright, L.L., 2007. Current and potential us corn stover supplies. *Agronomy Journal* 99, 1–11.
- He, E., Xie, Y., Liu, L., Chen, W., Jin, Z., Jia, X., 2023. Physics guided neural networks for time-aware fairness: an application in crop yield pre-

- diction, in: Proceedings of the AAAI Conference on Artificial Intelligence, pp. 14223–14231.
- He, K., Zhang, X., Ren, S., Sun, J., 2016. Deep residual learning for image recognition, in: Proceedings of the IEEE conference on computer vision and pattern recognition, pp. 770–778.
- Herzmann, D., Arritt, R., Todey, D., 2004. Iowa environmental mesonet. Available at mesonet. agron. iastate. edu/request/coop/fe. phtml (verified 27 Sept. 2005). Iowa State Univ., Dep. of Agron., Ames, IA .
- Hoerl, A.E., Kennard, R.W., 1970. Ridge regression: Biased estimation for nonorthogonal problems. *Technometrics* 12, 55–67.
- Hosseini, M., Kerner, H.R., Sahajpal, R., Puricelli, E., Lu, Y.H., Lawal, A.F., Humber, M.L., Mitkish, M., Meyer, S., Becker-Reshef, I., 2020. Evaluating the impact of the 2020 iowa derecho on corn and soybean fields using synthetic aperture radar. *Remote Sensing* 12, 3878.
- Huang, J., Wang, H., Dai, Q., Han, D., 2014. Analysis of ndvi data for crop identification and yield estimation. *IEEE Journal of Selected Topics in Applied Earth Observations and Remote Sensing* 7, 4374–4384.
- Huete, A., Didan, K., Miura, T., Rodriguez, E.P., Gao, X., Ferreira, L.G., 2002. Overview of the radiometric and biophysical performance of the modis vegetation indices. *Remote sensing of environment* 83, 195–213.
- Ines, A.V., Das, N.N., Hansen, J.W., Njoku, E.G., 2013. Assimilation of remotely sensed soil moisture and vegetation with a crop simulation model for maize yield prediction. *Remote Sensing of Environment* 138, 149–164.

- Johnson, D.M., 2014. An assessment of pre-and within-season remotely sensed variables for forecasting corn and soybean yields in the united states. *Remote Sensing of Environment* 141, 116–128.
- Jones, J.W., Hoogenboom, G., Porter, C.H., Boote, K.J., Batchelor, W.D., Hunt, L., Wilkens, P.W., Singh, U., Gijsman, A.J., Ritchie, J.T., 2003. The dssat cropping system model. *European journal of agronomy* 18, 235–265.
- Karpatne, A., Kannan, R., Kumar, V., 2022. Knowledge guided machine learning: Accelerating discovery using scientific knowledge and data. CRC Press.
- Kimball, B.A., Thorp, K.R., Boote, K.J., Stockle, C., Suyker, A.E., Evett, S.R., Brauer, D.K., Coyle, G.G., Copeland, K.S., Marek, G.W., et al., 2023. Simulation of evapotranspiration and yield of maize: An inter-comparison among 41 maize models. *Agricultural and Forest Meteorology* 333, 109396.
- Kingma, D.P., Ba, J., 2014. Adam: A method for stochastic optimization. arXiv preprint arXiv:1412.6980 .
- KRIEGLER, F.J., 1969. Preprocessing transformations and their effects on multispectral recognition, in: *Proceedings of the sixth international symposium on remote sensing of environment*, pp. 97–131.
- Kucharik, C.J., Ramankutty, N., 2005. Trends and variability in us corn yields over the twentieth century. *Earth Interactions* 9, 1–29.
- Licheng, L., Zhou, W., Jin, Z., Tang, J., Jia, X., Jiang, C., Guan, K., Peng,

- B., Xu, S., Yang, Y., et al., 2022. Estimating the autotrophic and heterotrophic respiration in the us crop fields using knowledge guided machine learning. Authorea Preprints .
- Licht, M., 2021. Corn and soybean planting date considerations. <https://crops.extension.iastate.edu/blog/mark-licht-zachary-clemens/corn-and-soybean-planting-date-considerations>.
- Lobell, D.B., Thau, D., Seifert, C., Engle, E., Little, B., 2015. A scalable satellite-based crop yield mapper. *Remote Sensing of Environment* 164, 324–333.
- Luo, Y., Liu, Q., Chen, Y., Hu, W., Tian, T., Zhu, J., 2023. Physics-guided discovery of highly nonlinear parametric partial differential equations, in: *Proceedings of the 29th ACM SIGKDD Conference on Knowledge Discovery and Data Mining*, pp. 1595–1607.
- Ma, Y., Zhang, Z., Kang, Y., Özdoğan, M., 2021a. Corn yield prediction and uncertainty analysis based on remotely sensed variables using a bayesian neural network approach. *Remote Sensing of Environment* 259, 112408.
- Ma, Y., Zhang, Z., Kang, Y., Özdoğan, M., 2021b. Corn yield prediction and uncertainty analysis based on remotely sensed variables using a bayesian neural network approach. *Remote Sensing of Environment* 259, 112408.
- Manual, A.B., 2013. *An introduction to statistical learning with applications in r* .
- McCown, R.L., Hammer, G.L., Hargreaves, J.N.G., Holzworth, D.P., Freebairn, D.M., 1996. Apsim: a novel software system for model development,

- model testing and simulation in agricultural systems research. *Agricultural systems* 50, 255–271.
- Mladenova, I.E., Bolten, J.D., Crow, W.T., Anderson, M.C., Hain, C.R., Johnson, D.M., Mueller, R., 2017. Intercomparison of soil moisture, evaporative stress, and vegetation indices for estimating corn and soybean yields over the us. *IEEE Journal of Selected Topics in Applied Earth Observations and Remote Sensing* 10, 1328–1343.
- Paszke, A., Gross, S., Massa, F., Lerer, A., Bradbury, J., Chanan, G., Killeen, T., Lin, Z., Gimelshein, N., Antiga, L., et al., 2019. Pytorch: An imperative style, high-performance deep learning library. *Advances in neural information processing systems* 32.
- Pedregosa, F., Varoquaux, G., Gramfort, A., Michel, V., Thirion, B., Grisel, O., Blondel, M., Prettenhofer, P., Weiss, R., Dubourg, V., Vanderplas, J., Passos, A., Cournapeau, D., Brucher, M., Perrot, M., Duchesnay, E., 2011. Scikit-learn: Machine learning in Python. *Journal of Machine Learning Research* 12, 2825–2830.
- Pignotti, G., Crawford, M., Han, E., Williams, M.R., Chaubey, I., 2023. Smap soil moisture data assimilation impacts on water quality and crop yield predictions in watershed modeling. *Journal of Hydrology* 617, 129122.
- Puntel, L.A., Sawyer, J.E., Barker, D.W., Dietzel, R., Poffenbarger, H., Castellano, M.J., Moore, K.J., Thorburn, P., Archontoulis, S.V., 2016. Modeling long-term corn yield response to nitrogen rate and crop rotation. *Frontiers in plant science* 7, 1630.

- Reichle, R., De Lannoy, G., Koster, R., Crow, W., Kimball, J., Liu, Q., Bechtold, M., 2022. Smap l4 global 3-hourly 9 km ease-grid surface and root zone soil moisture analysis update, version 7. URL: <http://nsidc.org/data/SPL4SMAU/versions/7>, doi:10.5067/LWJ6TF5SZRG3.
- Ridnik, T., Ben-Baruch, E., Zamir, N., Noy, A., Friedman, I., Protter, M., Zelnik-Manor, L., 2021. Asymmetric loss for multi-label classification, in: Proceedings of the IEEE/CVF international conference on computer vision, pp. 82–91.
- Schaaf, C., Wang, Z., 2015. Mcd43a4 modis/terra+ aqua brdf/albedo nadir brdf adjusted ref daily l3 global-500m v006. nasa eosdis land processes daac. USGS Earth Resources Observation and Science (EROS) Center, Sioux Falls, South Dakota (<https://lpdaac.usgs.gov>) .
- Schreiber-Gregory, D.N., 2018. Ridge regression and multicollinearity: An in-depth review. *Model Assisted Statistics and Applications* 13, 359–365.
- Shahhosseini, M., Hu, G., Huber, I., Archontoulis, S.V., 2021. Coupling machine learning and crop modeling improves crop yield prediction in the us corn belt. *Scientific reports* 11, 1606.
- Thompson, L.M., 1969. Weather and technology in the production of corn in the us corn belt 1. *Agronomy Journal* 61, 453–456.
- Unganai, L.S., Kogan, F.N., 1998. Drought monitoring and corn yield estimation in southern africa from avhrr data. *Remote sensing of environment* 63, 219–232.

- USDA, 2020. United states department of agriculture national agricultural statistics service .
- USDA, 2025. Crop calendars for united states. https://ipad.fas.usda.gov/rssiws/al/crop_calendar/us.aspx.
- USDA-NASS, C., 2017. Usda national agricultural statistics service cropland data layer .
- Van Diepen, C.v., Wolf, J.v., Van Keulen, H., Rappoldt, C., 1989. Wofost: a simulation model of crop production. *Soil use and management* 5, 16–24.
- Vaswani, A., 2017. Attention is all you need. arXiv preprint arXiv:1706.03762 .
- Vergopolan, N., Xiong, S., Estes, L., Wanders, N., Chaney, N.W., Wood, E.F., Konar, M., Caylor, K., Beck, H.E., Gatti, N., et al., 2021. Field-scale soil moisture bridges the spatial-scale gap between drought monitoring and agricultural yields. *Hydrology and Earth System Sciences* 25, 1827–1847.
- Wang, A.X., Tran, C., Desai, N., Lobell, D., Ermon, S., 2018. Deep transfer learning for crop yield prediction with remote sensing data, in: *Proceedings of the 1st ACM SIGCAS Conference on Computing and Sustainable Societies*, pp. 1–5.
- Wang, D., 2021. Modis/terra+qua surface radiation daily/3-hour l3 global 1km sin grid v061 [data set]. NASA EOSDIS Land Processes Distributed Active Archive Center. (<https://lpdaac.usgs.gov>) .

- Wang, J., Rich, P.M., Price, K.P., Kettle, W.D., 2005. Relations between ndvi, grassland production, and crop yield in the central great plains. *Geocarto International* 20, 5–11.
- Wang, X., Ma, Y., Xu, Y., Huang, Q., Yang, Z., Zhang, Z., 2025. Learning county from pixels: Corn yield prediction with attention-weighted multiple instance learning. *International Journal of Remote Sensing* , 1–31.
- Ward, M., 2023. 2023: A head-scratching year for missouri corn yields. <https://www.farmprogress.com/corn/2023-a-head-scratching-year-for-missouri-corn-yields>.
- Weiss, M., Baret, F., Garrigues, S., Lacaze, R., 2007. Lai and fapar cyclopes global products derived from vegetation. part 2: validation and comparison with modis collection 4 products. *Remote Sensing of Environment* 110, 317–331. URL: <https://www.sciencedirect.com/science/article/pii/S0034425707000910>, doi:<https://doi.org/10.1016/j.rse.2007.03.001>.
- Weiss, M., Baret, F., Leroy, M., Hauteceur, O., Bacour, C., Prevol, L., Bruguier, N., 2002. Validation of neural net techniques to estimate canopy biophysical variables from remote sensing data. *Agronomie-Sciences des Productions Vegetales et de l'Environnement* 22, 547–554.
- Weiss, M., Baret, F., Smith, G., Jonckheere, I., Coppin, P., 2004. Review of methods for in situ leaf area index (lai) determination: Part ii. estimation of lai, errors and sampling. *Agricultural and Forest Meteorology* 121, 37–53. URL: <https://www.sciencedirect.com/science/article/>

[pii/S0168192303001631](https://doi.org/10.1016/j.agrformet.2003.08.001), doi:<https://doi.org/10.1016/j.agrformet.2003.08.001>.

- Weiss, M., Jacob, F., Duveiller, G., 2020. Remote sensing for agricultural applications: A meta-review. *Remote sensing of environment* 236, 111402.
- Williams, J.R., Izaurralde, R.C., 2010. The apex model, in: *Watershed models*. CRC Press, pp. 461–506.
- Yang, Q., Liu, L., Zhou, J., Ghosh, R., Peng, B., Guan, K., Tang, J., Zhou, W., Kumar, V., Jin, Z., 2023. A flexible and efficient knowledge-guided machine learning data assimilation (kgml-da) framework for agroecosystem prediction in the us midwest. *Remote Sensing of Environment* 299, 113880.
- Yang, Q., Liu, L., Zhou, J., Rogers, M., Jin, Z., 2024. Predicting the growth trajectory and yield of greenhouse strawberries based on knowledge-guided computer vision. *Computers and Electronics in Agriculture* 220, 108911.
- You, J., Li, X., Low, M., Lobell, D., Ermon, S., 2017. Deep gaussian process for crop yield prediction based on remote sensing data, in: *Proceedings of the AAAI conference on artificial intelligence*.
- Zhen, X., Huo, W., Tian, D., Zhang, Q., Sanz-Saez, A., Chen, C.Y., Batchelor, W.D., 2023. County level calibration strategy to evaluate peanut irrigation water use under different climate change scenarios. *European Journal of Agronomy* 143, 126693.
- Zhen, X., Zhang, Q., Sanz-Saez, A., Chen, C.Y., Dang, P.M., Batchelor, W.D., 2022. Simulating drought tolerance of peanut varieties by maintaining photosynthesis under water deficit. *Field Crops Research* 287, 108650.